AIAA SciTech Forum
8–12 January 2018, Kissimmee, Florida
2018 AIAA/ASCE/AHS/ASC Structures, Structural Dynamics, and Materials Conference

10.2514/6.2018-0730

A study on the influence of fatigue damage initiation laws for cohesive zone models in propagation-driven load cases

Michael May[1]
Fraunhofer Institute for High-Speed Dynamics, Ernst-Mach-Institute, EMI, Eckerstraße 4, 79104 Freiburg, Germany

Paul W. Harper[2]
Advanced Composites Center for Innovation and Science, Queens Building, Bristol, BS81TR, UK

and

Stephen R. Hallett[3]
Advanced Composites Center for Innovation and Science, Queens Building, Bristol, BS81TR, UK

Cohesive zone models for composite laminates considering a Paris-law based damage function for fatigue are well established to model propagation of delamination from existing flaws. However, these models have some limitations in cases without an existing flaw. The limitations occurring in these special cases can be overcome by incorporating SN-curve based damage initiation laws. However, it has not yet been investigated if the combination of different damage models has a strong influence on scenarios with existing pre-cracks, such as typical linear elastic fracture mechanics specimens. Therefore, the 4ENF test is modeled with a propagation-only model and a combined initiation and propagation model. It is shown that the SN-curve based damage initiation model does not affect the Paris-law based damage propagation model negatively.

I. Nomenclature

α	=	exponent of mixed-mode cohesive law
C	=	coefficient for the Paris law
C_I	=	mode I coefficient for the Paris law
C_{II}	=	mode II coefficient for the Paris law
C_m	=	mixed-mode coefficient for the Paris law
$cosI$	=	direction cosinus for mode I loading
$cosII$	=	direction cosinus for mode II loading
D_{tot}	=	total damage
d_f	=	damage caused by fatigue loading
$d_{f,i}$	=	damage accumulated during fatigue damage initiation
$d_{f,u}$	=	correction term for unphysical damage accumulated during fatigue loading
d_s	=	damage caused by static loading
da	=	change of crack length
dd_f	=	change of fatigue damage
dN	=	change of fatigue cycles
dt	=	change of time
ΔG	=	variation of strain energy release rate during a fatigue load cycle
Δt	=	time step size
δ_m	=	current mixed-mode displacement

[1] Head of Department, Department of Materials and Simulation Methods, michael.may@emi.fraunhofe.de. AIAA member
[2] Teaching Fellow, Department of Aerospace Engineering, paul.harper@bristol.ac.uk.
[3] Professor in Composite Structures, Department of Aerospace Engineering, stephen.hallett@bristol.ac.uk.

$\delta_{m,0}$	=	mixed-mode displacement at damage initiation
E_{11}	=	Young's modulus in fiber direction
E_{22}	=	Young's modulus in 2-direction
E_{33}	=	Young's modulus in 3-direction
G_{12}	=	Shear modulus in 12-direction
G_{23}	=	Shear modulus in 23-direction
G_{31}	=	Shear modulus in 31-direction
G_I	=	current strain energy release rate in mode I
G_{Ic}	=	critical strain energy release rate in mode I
G_{II}	=	current strain energy release rate in mode II
G_{IIc}	=	critical strain energy release rate in mode II
G_{max}	=	maximum strain energy release rate
G_T	=	current mixed-mode strain energy release rate
K_I	=	mode I penalty stiffness for interface element
K_{II}	=	mode II penalty stiffness for interface element
L_{fat}	=	length of the cohesive zone under fatigue loading
Log	=	base 10 logarithm
m	=	exponent for the Paris law
m_I	=	mode I exponent for the Paris law
m_{II}	=	mode II exponent for the Paris law
m_m	=	exponent for the Paris law for a given mode-mixity
N	=	elapsed number of fatigue cycles
N_{ini}	=	number of fatigue cycles until damage initiation
ν_{21}	=	Poisson's ratio in 21-direction
ν_{31}	=	Poisson's ratio in 31-direction
ν_{32}	=	Poisson's ratio in 32-direction
s	=	slope of the SN-curve
s_I	=	slope of the SN-curve for pure mode I loading
s_{II}	=	slope of the SN-curve for pure mode II loading
σ	=	stress
σ_I	=	current interface element mode I stress
σ_I^{max}	=	interlaminar tensile strength
σ_{II}	=	current interface element mode II stress stress
σ_{II}^{max}	=	interlaminar shear strength
σ_m	=	interface element mixed-mode stress
σ^{max}	=	interface element mixed-mode stress at damage initiation
σ_{stat}	=	static failure stress
t	=	time

II. Introduction

FATIGUE loading has become one of the major design drivers in rotating components made from composite materials such as wind turbine blades, helicopter rotor blades, and engine fan blades. In recent years, there have been several efforts to describe the fatigue propagation of delamination in composites using cohesive zone models[1,2,3,4,5]. All of these methods describe crack propagation as a function of load cycles. Whilst all of these methods are able to predict propagation of an existing crack in composites under fatigue loading with reasonable accuracy[6], May and Hallett showed that these types of models fail to predict failure in cases without an initial pre-crack such as a Short Beam Shear test (SBS) or a Double Notched Shear test (DNS)[7]. In a recent review on methods for the prediction of fatigue delamination growth in composites, Pascoe et al.[8] pointed out that the main advantage of cohesive zone models compared to classical LEFM methods, the possibility for combined simulation of initiation and propagation of delamination in a single coherent analysis without the need for remeshing, was not exploited if cohesive zone models for fatigue featured only propagation criteria. Additionally, Quaresimin and Ricotta demonstrated that in some cases damage initiation could be a major part of total fatigue life[9]. The May-Hallett model[7,10] addresses this issue by combining SN-curve based damage initiation models with a Paris-law damage propagation law. The model was validated against experimental data by predicting SN-curves for matrix cracking in $[0_2,90_4]_s$ and $[0_2,60_4]_s$ specimens[11]. However, it remains an open question if these types of combined SN-curve based damage initiation and Paris-law based damage propagation laws could potentially cause inadvertent effects in propagation-dominated scenarios. This article addresses this question by modelling a propagation-only case with the propagation-based Harper-Hallett model[3] and its extension, the May-Hallett model[7,10] combining initiation and propagation models. The article is structured as follows: First, the model formulations are summarized. Then both models are used in the simulation of a 4ENF specimen subjected to fatigue loading at different levels of severity. The article closes with a discussion of the simulation results.

III. Model formulations

Both model formulations used here are extensions to the static bi-linear cohesive zone model developed by Jiang et al.[12] which employs a stress-based damage initiation criterion in the form of:

$$\sqrt{\frac{\max(\sigma_I,0)}{\sigma_I^{\max}}+\left(\frac{\sigma_{II}}{\sigma_{II}^{\max}}\right)^2}=1 \tag{1}$$

where σ_I is the normal interlaminar tensile stress, σ_{II} is the interlaminar shear stress, σ_I^{max} is the interlaminar tensile strength, σ_{II}^{max} is the interlaminar shear strength, and an energy based failure criterion in the form of:

$$\left(\frac{G_I}{G_{Ic}}\right)^{\alpha}+\left(\frac{G_{II}}{G_{IIc}}\right)^{\alpha}=1. \tag{2}$$

Here, G_I and G_{II} are the mode I and mode II energies associated with the current state of loading, G_{Ic} and G_{IIc} are the mode I and mode II fracture toughness, and α is an empirical parameter, typically in the range of 1 to 2.

This model was implemented in the explicit FE code LS-DYNA. More details on the implementation and the damage evolution under static loading can be found in the original article by Jiang et al.[12]. Fig. 1 illustrates the traction-separation law underlying both fatigue models. In the following description, the main features of the Harper-Hallett model[3] and the May-Hallett model[7,10] are summarized in order to enhance clarity of this investigation.

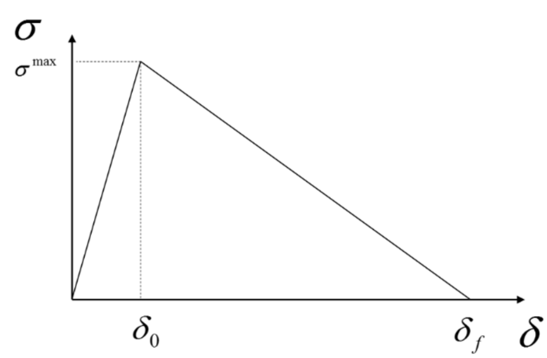

Figure 1: Bilinear traction-separation law used in both models.

A. The Harper-Hallett model

Since LS-DYNA is an explicit FE code is based in the time domain, the amount of damage accumulated in each time step is dependent on the stress state and the cycle frequency, dN/dt, which is defined as the number of elapsed fatigue cycles per second of LS-DYNA analysis time – the so-called pseudo-time. The crack propagation rate can be written in terms of pseudo-time:

$$\frac{da}{dt}=\frac{da}{dN}\cdot\frac{dN}{dt} \tag{3}$$

Similar to most fatigue damage propagation models, the Harper-Hallett model uses an adapted version of the Paris law in order to describe damage accumulation under high-cycle fatigue loading

$$\frac{da}{dN} = C \cdot (\Delta G)^m \tag{4}$$

For mixed-mode loading, the coefficients C and m are calculated following a mixed-mode law proposed by Blanco et al.[13].

$$\log C = \log C_I + \left(\frac{G_{II}}{G_T}\right) \cdot \log C_m + \left(\frac{G_{II}}{G_T}\right)^2 \cdot \log \frac{C_{II}}{C_m \cdot C_I} \tag{5}$$

$$m = m_I + m_m\left(\frac{G_{II}}{G_T}\right) + (m_{II} - m_I - m_m)\left(\frac{G_{II}}{G_T}\right)^2 \tag{6}$$

C_I, C_{II}, C_m, m_I, m_{II}, m_m are the Paris law coefficients and exponents for pure mode I, pure mode II and one mixed-mode load case, respectively.

Following Schön[14], the change in strain energy during each load cycle, ΔG, is expressed as a function of the maximum strain energy release rate, G_{max}, and the R-ratio R:

$$\Delta G = G_{\max} \cdot (1 - R^2). \tag{7}$$

The total damage D_{tot} is the sum of static damage d_s and accumulated fatigue damage d_f:

$$D_{tot} = d_s + d_f \quad . \tag{8}$$

For each model time step, the fatigue damage d_f is updated using:

$$d_f(t) = d_f(t - \Delta t) + \frac{dN}{dt} \cdot \Delta t \cdot \frac{dd_f}{dN} , \tag{9}$$

Where

$$\frac{dd_f}{dN} = \frac{1 - d_s - d_{f,u}}{L_{fat}} \cdot \frac{da}{dN} . \tag{10}$$

Here, L_{fat} is the cohesive zone length under fatigue loading and $d_{f,u}$ is a correction term explained by Harper and Hallett[3].

D_{tot} is used to update the interface strength after each time step

$$\sigma_m = \sigma^{\max} \cdot (1 - D_{tot}) . \tag{11}$$

The interface element fails once D_{tot} reaches a value of unity and the interface strength degrades to zero.

B. The May-Hallett model

The May-Hallett model is an extension to the Harper-Hallett model. The May-Hallett model combines the Paris-law based damage propagation model with an SN-curve based damage initiation model. This is motivated by the assumption that damage initiation in pristine composites is a material property of the resin[15,16]. In the May-Hallett model, the SN-curves for damage initiation are described by simple logarithmic functions:

$$\frac{\sigma}{\sigma_{stat}} = 1 - s \cdot \log N . \tag{12}$$

Here, σ/σ_{stat} is the applied stress divided by the static failure stress and is subsequently referred to as severity, s is the slope of the SN-curve, and N is the elapsed number of cycles. This approach has also recently been picked up by Fang et al.[17,18].

In cases of mixed-mode loading, we assume a simple quadratic relationship for determining the slope of the SN-curve

$$s = s_I \cdot (\cos I)^2 + s_{II} \cdot (\cos II)^2 . \tag{13}$$

Here, s_I, s_{II} are the slopes of the SN-curves for pure mode I and pure mode II loading, respectively; $\cos I$ and $\cos II$ are the direction cosines, defined by Jiang et al.[12].

The fatigue damage initiation variable is defined as

$$d_{f,i}(t) = d_{f,i}(t - \Delta t) + \frac{dN/dt}{1 \cdot 10^{\frac{1-(\sigma/\sigma_{stat})}{s}}} \cdot \Delta t . \tag{14}$$

It is important to note that in previous studies on the May-Hallett model[7], the fatigue damage initiation laws were – analogous to the quasi-static definition of initiation and propagation in cohesive interface elements – only applied on the linear elastic part of the traction-separation law. However, it was found that:

i. Unlike the quasi-static interpretation of damage initiation in cohesive interface elements, where damage starts accumulating once the maximum interface stress has been reached ($\delta = \delta_0$), under fatigue loading, damage initiation can occur for each loading state of the traction-separation law ($0 \le \delta < \delta_f$).
ii. Damage initiation is a non-local process, which is typically occurring at a length scale of several mm, spanning several interface elements.

May and Hallett[10] therefore developed a methodology to identify the location of damage initiation and simultaneously degrade all elements within a pre-defined area of influence, the so-called initiation size, which - for brittle materials such as carbon-epoxy composites - is typically of size 3 mm. The stresses in the interface elements within the initiation zone are updated as follows:

$$\sigma = \begin{cases} \sigma^{\max} \cdot \dfrac{\delta_m}{\delta_{m,0}} \cdot \max\left(0, \left(1 - \dfrac{N - N_{ini}}{1.01 \cdot N_{ini}}\right)\right) & for \quad d_s = 0 \\ \sigma^{\max} \cdot (1 - d_s) \cdot \max\left(0, \left(1 - \dfrac{N - N_{ini}}{1.01 \cdot N_{ini}}\right)\right) & for \quad 0 < d_s < 1 \end{cases} . \tag{15}$$

The first expression is used if the interface element is loaded on the linear-elastic part of the traction-separation law, the second expression is used if the interface element is loaded on the softening part of the traction-separation law. Here, δ_m is the mixed-mode displacement, $\delta_{m,0}$ is the mixed-mode displacement at damage initiation, N_{ini} is the number of cycles corresponding to damage initiation calculated by rearranging eq. (12)

$$N_{ini} = 1 \cdot 10^{\frac{1 - \sigma/\sigma_{stat}}{s}} . \tag{16}$$

IV.Modeling of a propagation-driven test case

A typical propagation case is modelled to investigate if the extension of the propagation based Harper-Hallett model with an SN-curve based damage initiation criterion has any negative effects on the prediction of propagation based load cases. The Four Point End Notched Flexure (4ENF)[19] was selected for this purpose. This test is commonly used to determine the quasi-static fracture toughness and fatigue crack growth rates in composite materials under pure shear loading[20,21]. A pre-cracked composite beam is loaded in a four point bending configuration resulting in stable mode II crack propagation of the initial pre-crack[22].

C. Model setup

Harper and Hallett[3] used experimental 4ENF data for HTA/6376C carbon/epoxy composites, taken from Asp et al.[21] to validate the Harper-Hallett model. As the Harper-Hallett model was already validated against experimental 4ENF data, the model can be taken as a reference for the May-Hallett model. The same FE mesh used by Harper and Hallett[3] was used here in order to eliminate discrepancies caused by mesh effects or boundary conditions. The model consists of a composite beam of length 150 mm, width 10 mm and thickness 3.2 mm, built from hexahedral solid elements with reduced integration and a rigid body loading bar of length 90 mm and width 10 mm. The beam was discretized by 1 element across the width, 6 elements through the thickness (allowing for bending), and an element length of 0.25 mm in the beam length direction. An orthotropic linear-elastic material model was applied to the beam. Considering the findings of Wisnom and Chang[23] with respect to the thickness of the resin rich layer between two composite plies, interface elements of thickness 0.005 mm were inserted in the mid-plane of the composite beam, thus allowing modeling of the delamination growth under loading. No interface elements were inserted over a length of 35 mm from the left end of the beam in order to create the required pre-crack. The Harper-Hallett model and the May-Hallett model were applied to the cohesive interface elements in separate simulations. Pinned boundary conditions were applied on either end of the beam. Contacts were created between the rigid loading roller and the composite beam as well as between the surfaces of the initial delamination, avoiding penetration problems during the simulation. The timestep of the explicit analysis was increased by artificially increasing the density of the finite elements to reduce run time, whilst ensuring that kinetic energy in the system was negligible compared to the total energy of the simulation model. Table 1 summarizes the material properties assigned to the continuum elements.

Table 1: Ply continuum element properties of HTA/6376C carbon/epoxy[3]

$E_{11}(GPa)$	$E_{22}=E_{33}(GPa)$	$G_{12}=G_{31}(GPa)$	$G_{23}(GPa)$	$\nu_{21}=\nu_{31}(-)$	$\nu_{32}(-)$
120	10.5	5.25	3.48	0.02625	0.51

All ply continuum elastic properties are given in the principal material coordinates 1,2,3. E_{11}, E_{22}, E_{33} are the Young's moduli, G_{12}, G_{31}, G_{23} are the shear moduli, ν_{21}, ν_{31}, ν_{32} are the Poisson's ratios.
Table 2 summarizes the interface element properties for HTA/6376C.

Table 2: Interface element properties for HTA/6376C carbon/epoxy.

$G_{Ic}(kJ/m^2)$	$C_I(mm/cycle)$	$m_I(-)$	$s_I(MPa/decade)$	$\sigma_I^{max}(MPa)$	$K_I(N/mm^3)$
0.26[3]	0.00651[3]	5.29[3]	0.072[24]	30[3]	100,000[3]
$G_{IIc}(kJ/m^2)$	$C_{II}(mm/cycle)$	$m_{II}(-)$	$s_{II}(MPa/decade)$	$\sigma_{II}^{max}(MPa)$	$K_{II}(N/mm^3)$
1.002[3]	0.0669[3]	9.6[3]	0.115[25]	60[3]	100,000[3]

G_{Ic}, G_{IIc}, C_I, C_{II}, m_I, m_{II}, σ_I, σ_{II}, σ_{Imax}, σ_{IImax}, K_I, K_{II} are the fracture toughness, Paris-law coefficients, Paris law exponents, SN-curve slope parameters, maximum stress of the interface element and the slope of the linear-elastic part of the traction-separation law for pure mode I and pure mode II, respectively. May et al.[11] recommended to extract the slope of the mode I and mode II SN-curves from transverse tension fatigue tests on thick UD composite beams and double notched shear tests, respectively. However, as no initiation data was available for HTA/6376C, the shapes of the SN-curves for damage initiation were assumed to be the same as for IM7/8552, which is currently the only material available that has been extensively characterized with respect to fatigue damage initiation.
To begin with, the FE model was loaded under displacement control in order to determine the quasi-static load corresponding to the onset of propagation of the initial delamination. For subsequent simulations, the prescribed displacement was removed and replaced by a prescribed load. It should be noted that the load is not modelled on a cycle-by cycle basis. Instead, only the envelope of the load is modelled, resulting in a higher numerical efficiency. This cycle-jump strategy is enabled by eq. (3). Three different severities relative to the static propagation load were assessed: 60%, 50% and 40% of the static propagation load. Following previous recommendations[10,25,26], the size of the initiation zone was chosen as 3.0 mm.

V.Results and Discussion

Figure 2 illustrates that the May-Hallett model correctly predicts the location of damage initiation adjacent to the pre-crack. The element highlighted in red is the interface element with the highest failure index, following the definition given by the authors in the original paper[10]. The elements in green are inside the damage initiation zone. Elements marked in blue are outside the damage initiation zone.

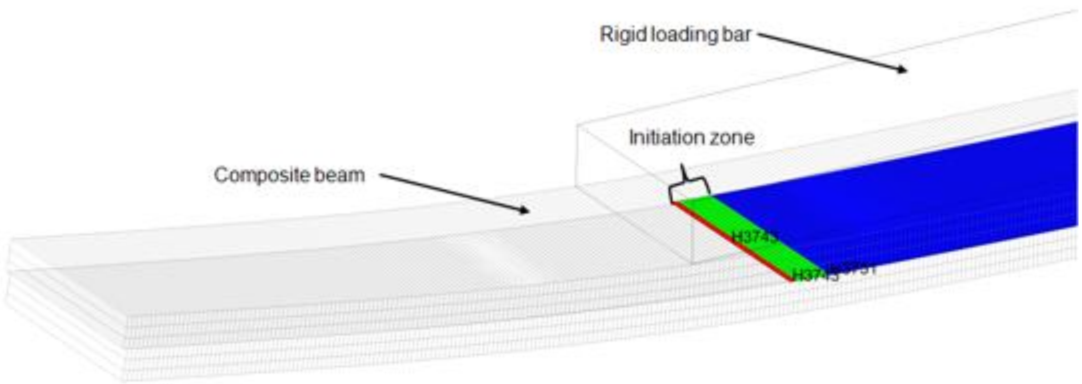

Figure 2: predicted location of damage initiation zone in 4ENF simulation.

In addition to this qualitative identification of the correct location of the onset of delamination, it is important to assess the subsequent propagation of delamination. Figures 3-5 compare the predicted crack lengths at several discrete numbers of cycles for the Harper-Hallett model (red triangles) and the May-Hallett model (blue diamonds) for 60%, 50% and 40% of the static propagation load.

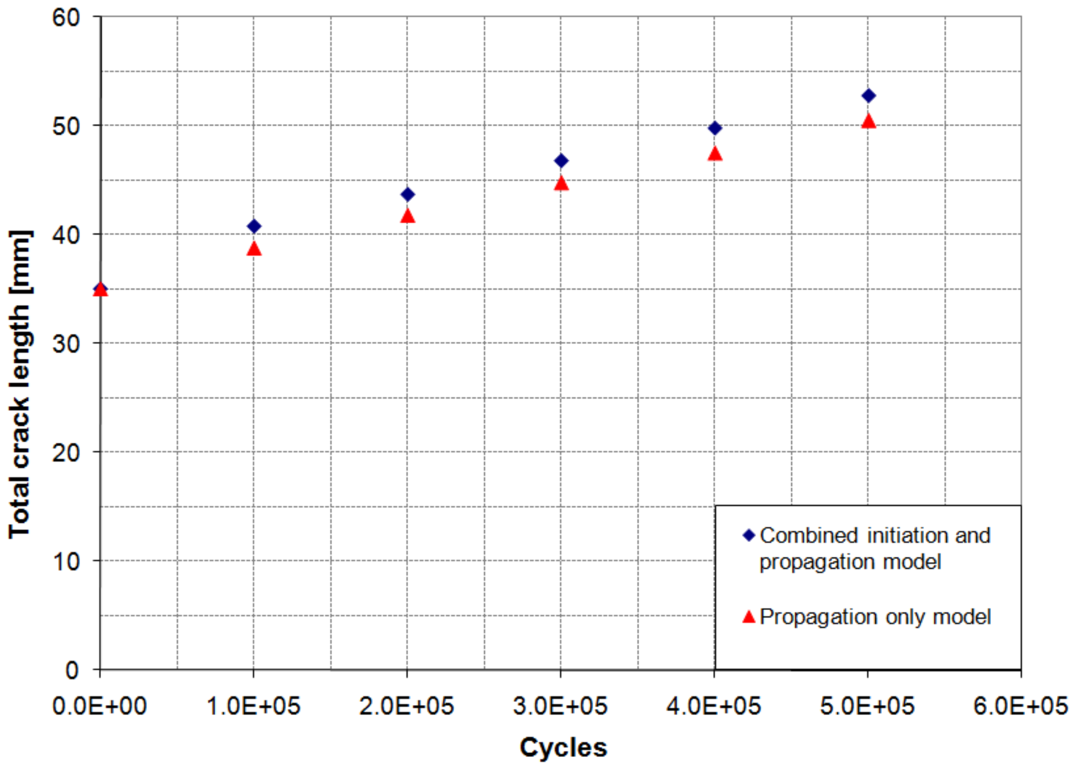

Figure 3: FE predictions for the 4ENF test, loaded at 60% of the static propagation load.

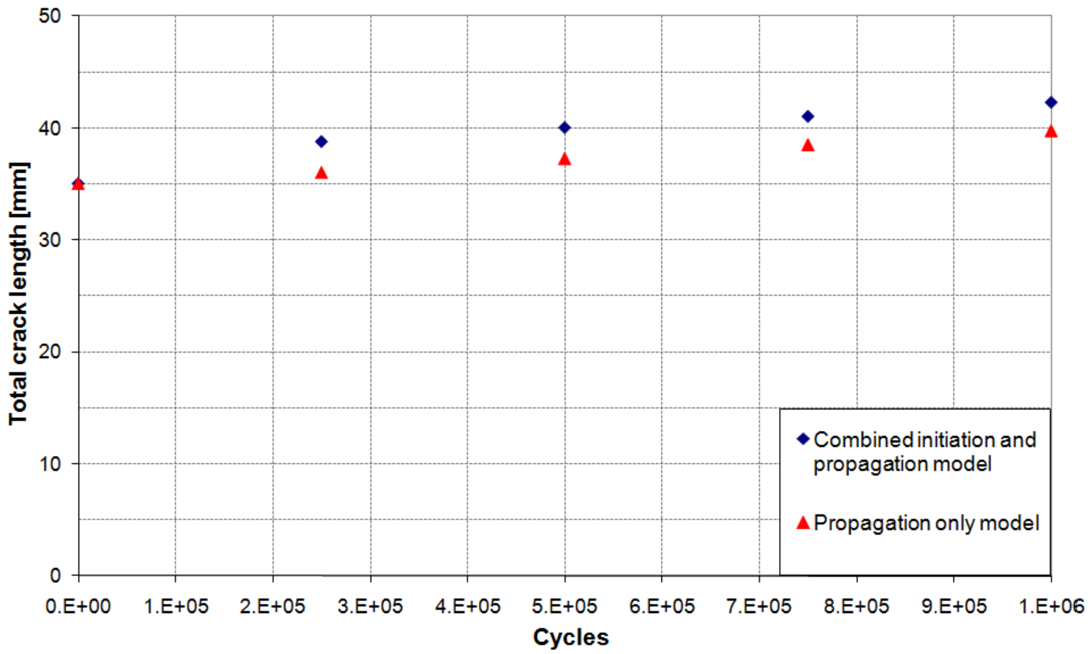

Figure 4: FE predictions for the 4ENF test, loaded at 50% of the static propagation load.

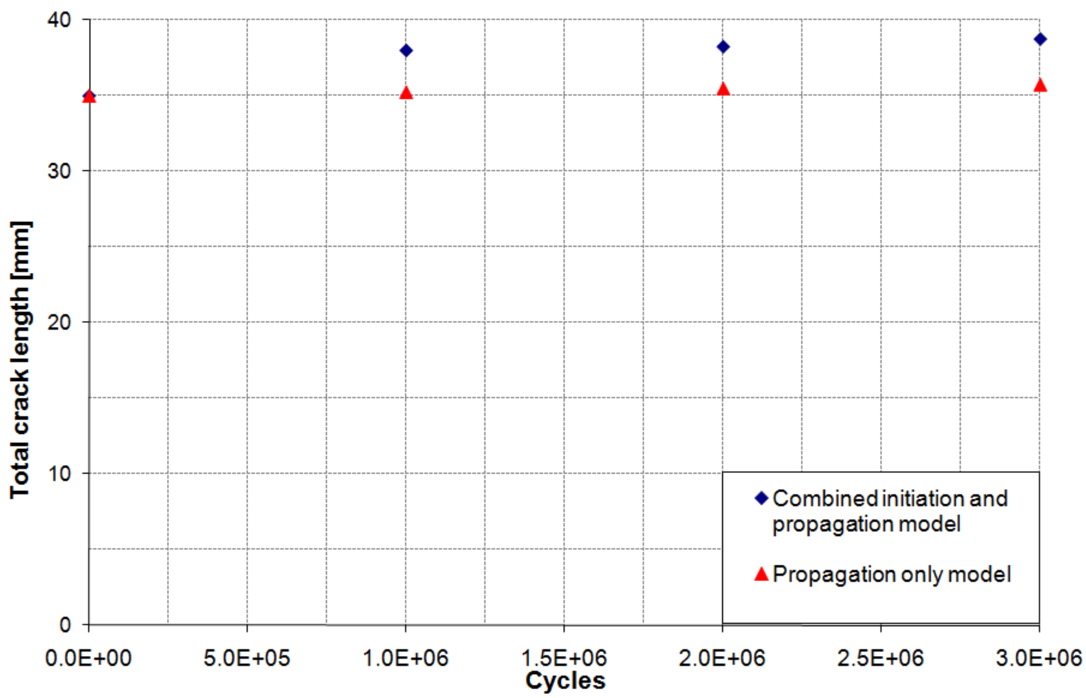

Figure 5: FE predictions for the 4ENF test, loaded at 40% of the static propagation load.

The predictions obtained from the May-Hallett model differ only slightly from the predictions obtained from the Harper-Hallett model. For a severity of 60%, the total crack length predicted by the May-Hallett model is on average 2 mm longer than the crack length predicted by the Harper-Hallett model. This difference is a consequence of the introduction of an initiation zone of length 3 mm. The May-Harper model predicts simultaneous failure of all elements within this initiation zone whilst for the same number of load cycles, the Paris-law based Harper-Hallett model propagates the crack by only 1 mm. Subsequently, both models predict stable crack growth at the same rate. Consequently, the initial difference in crack length of approximately 3mm remains constant. The predicted crack lengths after 500,000 load cycles are 52.8 mm and 50 mm, respectively. Similar behavior is observed for 50% severity and 40% severity. After 106 load cycles at a severity of 50%, the Harper-Hallett model predicts a crack length of 40 mm; the May-Hallett model predicts a crack length of 42.5 mm. After $3x10^6$ load cycles at a severity of 40%, the Harper-Hallett model predicts a crack length of 35.8 mm, the May-Hallett model predicts a crack length of 38.5 mm. As expected, the reduction of the applied load results in a slower crack growth rate. The crack growth rates can be extracted from the three previous graphs by dividing the difference in crack length between two data points by the number of elapsed cycles. For example, for the applied severity of 60% of the static propagation load, the crack grows at a steady rate of $3.0x10^{-5}$ mm/cycle. The crack growth rates for severities of 50% and 40% of the static propagation load are $5.0x10^{-6}$ mm/cycle and $2.5x10^{-7}$ mm/cycle respectively. Figure 6 shows no difference in the predicted crack growth rates between the Harper-Hallett propagation model and the May-Hallett initiation and propagation model once the cracks have started to grow for the severities of 60% and 50% of the static load and only a small difference for a severity of 40% of the static load.

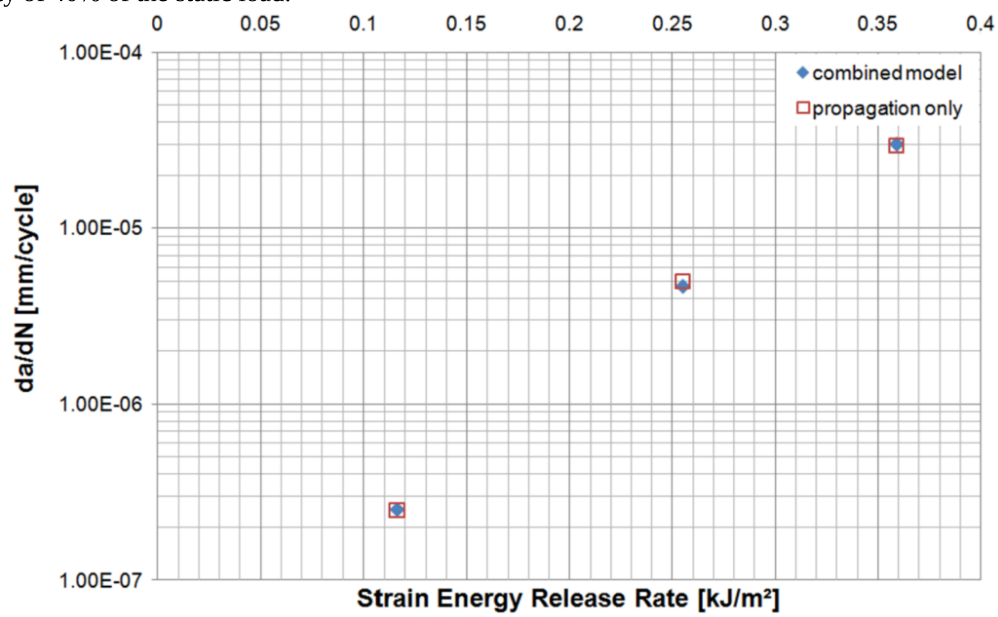

Figure 6: Paris curves extracted from the 4ENF simulations.

VI. Conclusions

The performance of two types cohesive zone models for predicting fatigue delamination in composites was compared. The Harper-Hallett model[3] was taken as a reference for Paris-law based propagation models. The May-Hallett model[7,10] was taken as a reference for combined fatigue damage initiation (based on SN-curves) and propagation (based on the Paris law) models. The reference test case was the propagation-driven 4ENF test In summary, the following conclusions can be drawn:

- The combined initiation and propagation model (May-Hallett model) predicts slightly longer crack lengths than the Harper-Hallett model. This is caused by the non-local approach describing a damage initiation zone of length 3 mm. The number of cycles until failure of the elements within this initiation zone, predicted by the SN-curve based damage initiation model, is shorter than the number of cycles required to advance the existing crack by 3 mm using the Paris law. Consequently, crack growth starts slightly earlier when using the May-Hallett model compared to the Harper-Hallett model.
- After initiation of crack propagation, both models predict the same crack growth rate.
- Despite the earlier start of damage propagation, the SN-curve based damage initiation law does not have any negative effects on the overall model response
- The results predicted by the May-Hallett model are conservative.

These findings demonstrate that cohesive zone models considering SN-curve based fatigue damage initiation laws, such as the May-Hallett model or the Fang-Cui-Lua model[17,18] can also be applied in propagation-driven load cases.

VII. Acknowledgments

The authors express their gratitude to Great Western Research, Rolls-Royce plc and Leonardo Helicopter Division (formerly Augusta Westlands) for funding this research.

VIII. References

[1]Robinson, P., Galvanetto, U., Tumino, D., and Belucci, G., “Numerical simulation of fatigue-driven delamination using interface elements,” *Int J Numer Meth Eng*, Vol. 63, No. 13, 2005, pp. 1824-1848.

[2]Turon, A., Costa, P., Camanho, P., and Dávila, C.,” Simulation of delamination in composites under high-cycle fatigue,” *Compos Part A - Appl S*, Vol. 38, No. 11, 2007, pp. 2270-2282.

[3]Harper, P. and Hallett, S., “A fatigue degradation law for cohesive interface elements - Development and application to composite materials,” *Int J Fatigue*, 2010, Vol. 32, No. 11, pp. 1774-1787.

[4]Kawashita, L. and Hallett, S., “A crack tip tracking algorithm for cohesive interface element analysis of fatigue delamination propagation in composite materials,” *Int J Solids Struct*, 2012, Vol. 49, No. 21, pp. 2898-2913.

[5]Bak, B, Turon, A., Lindgaard, E., and Lund, E., “A Simulation Method for High-Cycle Fatigue-Driven Delamination using a Cohesive Zone Model,” *Int J Numer Meth Eng*, 2016, Vol. 106, No. 3, pp. 163-191.

[6]Bak, B., Turon, A., Lindgaard, E., and Lund, E., “A Benchmark Study on Simulation Methods for High-Cycle Fatigue-Driven Delamination Based on Cohesive Zone Models,” *Compos Struct*, 2017, Vol. 164, pp. 198-206.

[7]May, M., and Hallett, S., “A combined model for initiation and propagation of damage under fatigue loading for cohesive interface elements,” *Compos Part A - Appl S*, 2010, Vol. 41, No. 12, pp. 1787-1796.

[8]Pascoe, J., Alderliesten, R., and Benedictus, R., “Methods for the prediction of fatigue delamination growth in composites and adhesive bonds - A critical review,” *Eng Fract Mech*, 2013, Vol. 112-113, pp. 72-96.

[9]Quaresimin, M., and Ricotta, M., “Fatigue behaviour and damage evolution of single lap bonded joints in composite materials”, *Compos Sci Technol*, 2006, Vol. 66, No. 2, pp.167-187.

[10]May, M., and Hallett, S., “An advanced model for initiation and propagation of damage under fatigue loading - part I: Model formulation,” *Compos Struct*, 2011, Vol. 93, No. 9, pp.2340-2349.

[11]May, M., Pullin, R., Eaton, M., Featherston, C., and Hallett, S., “An advancd model for initiation and propagation of damage under fatigue loading - part II: Matrix cracking validation cases,” *Compos Struct*, 2011, Vol. 93, No. 9, pp.2350-2357.

[12]Jiang, W., Hallett, S., Green, B., and Wisnom, M., “A concise interface constitutive law for analysis of delamination and splitting in composite materials and its application to scaled notched tensile specimens,” *Int J Numer Meth Eng*, 2007, Vol. 69, No. 9, pp. 1982-1995.

[13]N. Blanco, E. Gamstedt, L. Asp and J. Costa, "Mixed-mode delamination growth in carbon-fibre composite laminates under cyclic loading," Int J Solids Stuct, pp. 4219-4235, 2004.

14J. Schön, "A model of fatigue delamination in composites," *Compos Sci Technol*, pp. 553-558, 2000.

[15]M. May and S. Hallett, "Damage initiation in polymer matrix composites under high-cycle fatigue loading - A question of definition or a material property?," *Int J Fatigue*, pp. 59-62, 2016.

[16]D. Krause, "A physically based micromechanical approach to model damage initiation and evolution of fiber reinforced polymers under fatigue loading conditions," Compos Part B - Eng, pp. 167-195, 2016.

[17]E. Fang, X. Cui, J. Lua, “An integrated crack initiation and propagation module for fatigue damage prediction of composite structures” Proceedings of the 58th AIAA/ASCE/AHS/ASC Structures, Structural Dynamics, and Materials Conference, 2017.

[18]E. Fang, X. Cui, J. Lua, “A continuum damage and discrete crack-based approach for fatigue response and residual strength prediction of notched laminated composites”, *J Compos Mater*, Vol 51, No. 15, 2017, pp.2203-2225.

[19]J. Reeder, K. Demarco and K. Whitley, "The use of doubler reinforcement in delamination toughness testing," *Compos Part A - Appl S*, pp. 1337-1344, 2004.

[20]P. Hansen and R. Martin, "DCB, 4ENF and MMB Delamination Characterisation of S2/8552 and IM7/8552," Materials Engineering Research Laboratory ltd, Herteford, Final Technical Report 1999/004057, 1999.

[21]L. Asp, A. Sjogren and E. Greenhalg, "Delamination Growth and Threshold in a Carbon/Epoxy Composite Under Fatigue Loading," *Journal of Composites Technology and Research*, pp. 55-68, 2001.

[22]C. Schuecker and B. Davidson, "Evaluation of the accuracy of the four-point bend end-notched flexure test for mode II delamination toughness determination," *Compos Sci Technol*, pp. 2137-2146, 2000.

[23]M. Wisnom and F. Chang, "Modelling of splitting and delamination in notched cross-ply laminates," *Compos Sci Technol*, pp. 2849-2856, 2000.

[24]T. O'Brien, A. Chawan, R. Krueger and I. Paris, "Transverse tension fatigue life characterizaion through flexure testing of composite materials," *Int J Fatigue*, pp. 127-145, 2002.

[25]M. May and S. Hallett, "An assessment of through-thickness shear tests for initiation of fatigue failure," *Compos Part A - Appl S*, pp. 1570-1578, 2010.

[26]W. Fricke and A. Müller-Schmerl, "Consideration of Crack Propagation Behaviour in the Design of Cyclic Loaded Structures," in Fatigue Design and Reliability, G. Marquis and J. Solin, Eds., 1998, pp. 163-172.